FULL PAPERS

Designer Nanorings with Functional Cavities from Self-Assembling β-Sheet Peptides

Il-Soo Park,[a] You-Rim Yoon,[a] Minseon Jung,[b] Kimoon Kim,[b] SeongByeong Park,[c] Seokmin Shin,[c] Yong-beom Lim,*[d] and Myongsoo Lee*[a]

Dedicated to Professor Eiichi Nakamura on the occasion of his 60th birthday

Abstract: β-Barrel proteins that take the shape of a ring are common in many types of water-soluble enzymes and water-insoluble transmembrane pore-forming proteins. Since β-barrel proteins perform diverse functions in the cell, it would be a great step towards developing artificial proteins if we can control the polarity of artificial β-barrel proteins at will. Here, we describe a rational approach to construct β-barrel protein mimics from the self-assembly of peptide-based building blocks. With this approach, the direction of the self-assembly process toward the formation of water-soluble β-barrel nanorings or water-insoluble transmembrane β-barrel pores could be controlled by the simple but versatile molecular manipulation of supramolecular building blocks. This study not only delineates the basic driving force that underlies the folding of β-barrel proteins, but also lays the foundation for the facile fabrication of β-barrel protein mimics, which can be developed as nanoreactors, ion- and small-molecule-selective pores, and novel antibiotics.

Keywords: nanostructures · peptides · protein folding · proteins · self-assembly

Introduction

In recent years, an interest in manmade or artificial bionanostructures, including peptide-based self-assembled nano-structures,[1–4] has been intense and is expected to escalate further.[2,3,5–7] Artificial bionanostructures can mimic or even have enhanced functional properties over the bionanostructures of biological origin (e.g., proteins and many subcellular organelles). Moreover, we can expect that artificial bionanostructures would have properties that are unprecedented in nature. Since the major driving force that underlies the formation of bionanostructures is a noncovalent self-assembly process, elaborately designed synthetic self-assembly building blocks should be one of the most suitable candidates for the construction of artificial bionanostructures.

β-Barrel proteins are commonly found in many cytoplasmic and transmembrane proteins. Cytoplasmic β-barrel proteins are water-soluble, whereas transmembrane β-barrel proteins are water-insoluble amphiphiles. Two of the most well-known examples of water-soluble β barrels are triosephosphate isomerase (TIM) barrel folds and β-barrel folds of a green fluorescent protein family.[8] Transmembrane β-barrel proteins are typically found in porins and other proteins that span cell membranes.[9] There is a variety of functions that transmembrane β-barrel proteins can perform, and the functional categories are still expanding. Structurally, a β barrel is a closed structure in which the first and the last β strands in a polypeptide chain are hydrogen-bonded

[a] I.-S. Park, Y.-R. Yoon, Prof. M. Lee
Center for Supramolecular Nano-Assembly
and Department of Chemistry, Seoul National University
Seoul 151-747 (Korea)
Fax: (+82)2-889-1568
E-mail: myongslee@snu.ac.kr

[b] M. Jung, Prof. K. Kim
Center for Smart Supramolecules and Department of Chemistry
Pohang University of Science and Technology
Pohang 790-784 (Korea)

[c] S. Park, Prof. S. Shin
Department of Chemistry, Seoul National University
Seoul 151-747 (Korea)

[d] Prof. Y.-b. Lim
Translational Research Center for Protein Function Control
and Department of Materials Science and Engineering
Yonsei University, Seoul 120-749 (Korea)
Fax: (+82)2-312-5375
E-mail: yblim@yonsei.ac.kr

⊡ Supporting information for this article is available on the WWW under http://dx.doi.org/10.1002/asia.201000428.

in an end-to-end manner. β strands in β-barrel proteins are typically arranged in an antiparallel fashion.

Inspired by the transmembrane β barrels of biological origin, many synthetic β-barrel-like assemblies have been developed. Noteworthy examples include *p*-oligophenyl rod-based β-barrel systems,[10–12] β-barrel helical pores from amphiphilic dendritic peptides,[13–15] β-sheet nanotubes from cyclic peptides,[16] and supramolecular barrels from amphiphilic rigid–flexible macrocycles.[17] These synthetic molecules have shown the possibilities of constructing artificial membrane pores or channels; however, their chemical components and self-assembled structures are largely different from those of natural β-barrel folds. In natural β-barrel folds, β strands are composed of natural amino acids and lie roughly parallel to the lipid bilayer membrane normal and span the entire thickness of the membrane.[9] Herein, we describe the development of β-barrel protein mimics of dual functionality through a β-sheet-forming peptide self-assembly. The most unique feature of this system is the formation of highly uniform and discrete water-soluble β-barrel nanoring structures with a hydrophobic interior that is highly similar to natural β-barrel proteins in structure and composition, which can in turn be transformed into transmembrane β-barrel pores by the simple manipulation of their molecular structure.

Results and Discussion

The β-sheet ribbons are organized in such as way that each β strand runs perpendicular to the 1D ribbon axis, which is called a cross-β structure.[18,19] β barrels are in fact ring-shaped nanostructures. To probe the structural requirements for β-sheet peptide nanoring formation, we set out to find a fundamental design principle for constructing nanoring structures from β-sheet peptides. Considering the fact that nanorings are highly curved structures, we hypothesized that the induction of curvature between the adjacent β strands would force the 1D structure to bend. On the basis of this hypothesis, we designed T-shape β-sheet peptide building blocks, thus anticipating that bulky hydrophilic dendrons placed at the central part of β-sheet-forming peptides might induce curvature at the interface between β strands (Figure 1 and the Supporting Information).

The organic/peptide hybrid T-shape building blocks consist of a β-sheet-forming peptide and a hydrophilic oligoether dendron. The dendron is symmetrically placed on the side face of the peptide backbone. The artificially designed β-sheet peptide has a repeating structure of hydrophobic (tryptophan), positively charged (lysine), hydrophobic (tryptophan), and negatively charged (glutamic acid) amino acids, which has been found to promote the correct hydrogen-bonding arrangement for β-sheet formation.[2,20–22] The building blocks were synthesized by a solid-phase peptide synthesis (SPPS) method with the combination of both natural amino acids and a modified amino acid. The modified amino acid was made from L-tyrosine, in which a bulky and hydrophilic oligoether dendron was attached to the side-chain phenol group. As the tyrosine derivative was prepared as an *N*-α-Fmoc-protected (Fmoc = 9-fluorenylmethoxycarbonyl) amino acid, it could be incorporated into the growing peptide chain by using standard Fmoc SPPS protocols.

Self-Assembling Peptide Nanorings in Aqueous Solution

To investigate the effect of bulky dendron placement within the β-sheet-forming peptide, we first synthesized and tested peptide **T3** (Figure 1). A notable structural feature of peptide **T3** is the presence of a second-generation triethylene glycol dendrimer at the central part of the peptide building block. As the dendron is much bulkier than the β strand (see the side view of peptide **T3** in Figure 1), we anticipated that the bulky dendrons would create the curvature at the interface between each building block owing to the steric repulsion between the dendritic chains. This building block is quite different from block conjugates of polyethylene glycol (PEG) and peptide since the ethylene glycol units of precisely defined molecular structure are placed in the middle of the peptide segment.[23,24]

Investigation by circular dichroism (CD) spectroscopy showed that peptide **T3** forms β-sheet structures in aqueous solutions (see the Supporting Information). The self-assembled morphology of peptide **T3** was visualized by transmission electron microscopy (TEM). Remarkably, peptide **T3** formed discrete nanoring structures (Figure 1 b and the Supporting Information). Every nanostructure has the shape of a nanoring, thereby indicating that the formation of nanorings from peptide **T3** is a highly efficient process. The nanoring diameter is highly uniform (≈ 11 nm), thereby indicating that there is a preferred geometrical packing requirement for nanoring formation. The cross-section of nanorings was about 4 nm, which corresponds well with the width of fully extended peptide **T3** (3.8 nm by the Corey–Pauling–Koltun (CPK) model; see Figure 1 d). Therefore, these results suggest that the nanorings are composed of a single layer of building blocks, with the β strands oriented perpendicular to the plane of the nanoring to be accommodated into a highly bent structure. A recent theoretical study in the gas phase, which has suggested that the rolling up of a β-sheet can drive the formation of a β barrel,[25,26] further supports this view. This finding, together with the uniform nanoring size, suggests that nanorings have been formed by end-to-end connection of β strands similarly to natural β-barrel proteins.

Consistent with these observations, structure modeling by molecular dynamics (MD) revealed that an approximately 11 nm-sized nanoring is the most stable structure for the peptide **T3** aggregates (Figure 1 e). The configurations for **T3** and the minimized structure of the 40-mer toroidal structure are shown in Figure 1 e. For smaller toroidal structures (i.e., 12-mer and 24-mer), it was found that their initial structures became unstable and were broken within 100 ps MD simulations at 300 K. For the 40-mer of **T3**; however, the toroidal pore structure was found to be stable and main-
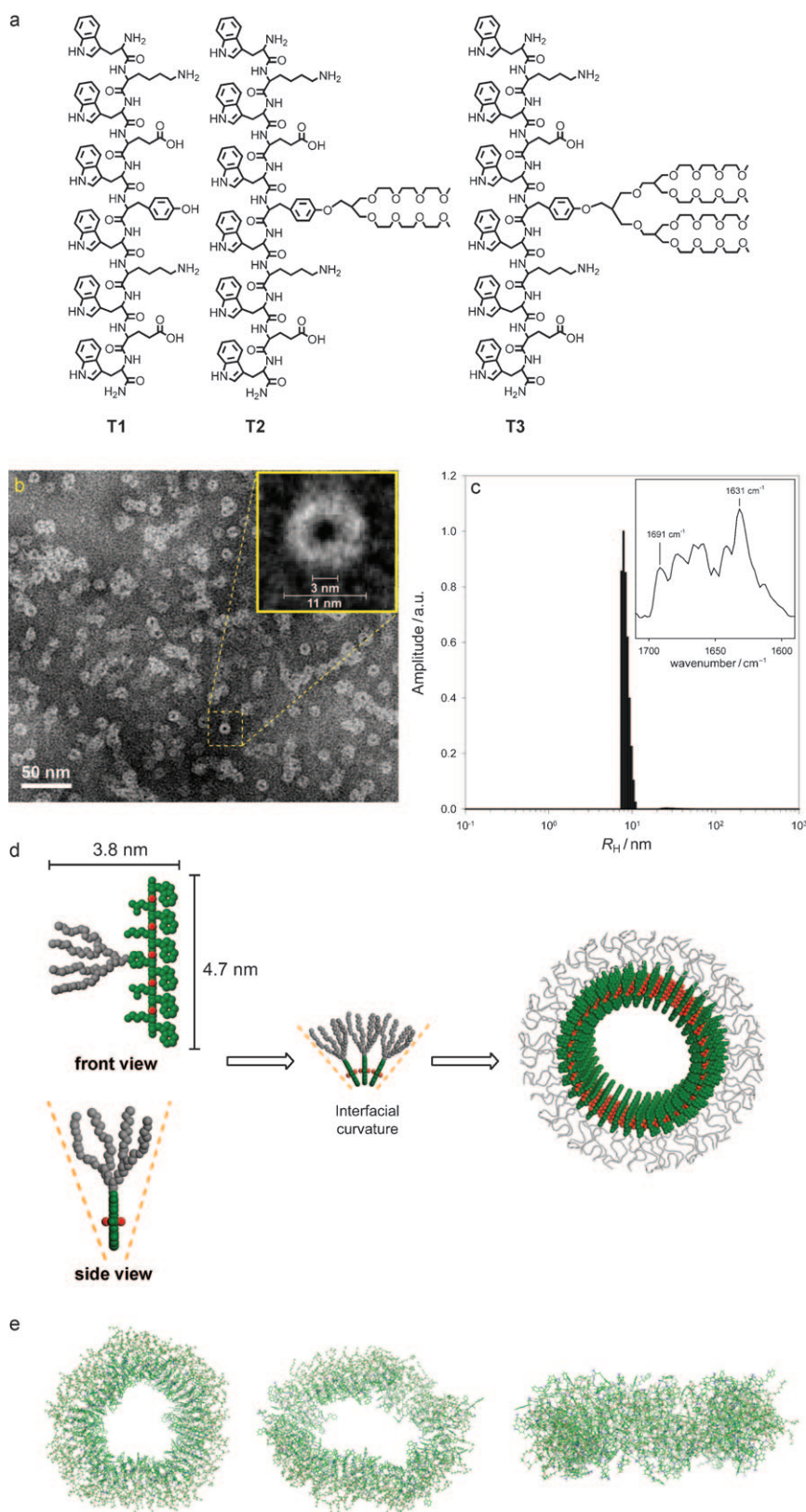
Figure 1. a) Structures of T-shape peptides. b) Negative-stain TEM image of peptide **T3** in 20 mM KF. c) Hydrodynamic radius distribution of peptide **T3** (20 μM) aggregates in 20 mM KF. Inset: FTIR spectrum of peptide **T3**. d) Corey–Pauling–Koltun (CPK) model of peptide **T3** and the model of self-assembled β barrels. e) MD simulation of **T3**. Minimized structure of the 40-mer **T3** β barrels (left). Top view (middle) and side view (right) of the resulting structure after 1 ns MD simulation.

tained its structure up to 1 ns of MD simulations. The simulation shows that the diameter for the inner pore is 3.5–4.5 nm, whereas the whole structure has the diameter of about 11 nm and thickness of about 4 nm, which is consistent with the experimental observations. More detailed simulation results will be published elsewhere.

To corroborate the notion that nanorings have not been formed during solvent evaporation process or by staining reagent while preparing the TEM samples on a grid, cryo-TEM and dynamic light scattering (DLS) experiments were performed. A cryo-TEM image in the Supporting Information shows dark toroidal objects of peptide **T3** against the vitrified solution background, thereby confirming that toroids have been formed in bulk solution. DLS experiments further corroborated this result. The DLS result shows the formation of nano-objects with a hydrodynamic radius (R_H) centered at 7.5 nm (Figure 1c). The small difference in the aggregate size between DLS and negative-stain TEM data is likely as a result of the samples being hydrated under the solution condition of DLS, whereas the sample is in a dried state during negative-stain TEM investigation. The inset in Figure 1c shows the FTIR spectrum of peptide **T3**. The presence of amide I contours for the β-sheet doublet at 1631 and 1691 cm^{-1} reveals that the β-sheet structure is in an antiparallel conformation within the nanorings.[27] All these data support the conclusion that peptide **T3** forms stable and water-soluble β-barrel nanorings. Considering the fact that β strands are in fact tilted with respect to the barrel axis in natural β-barrel proteins, β strands in the peptide nanorings are also likely to

be tilted to form flat β sheets. More in-depth atomic-level structural studies should be the subject of the further research.

Structural Requirements for Nanoring Formation

To gain further insight into the structural requirement for nanoring formation, we synthesized analogous T-shape peptides (**T1**, **T2**, and **T4**) while varying the relative volume fraction (f) of a dendron to a β-sheet peptide. As peptide **T1** contains an unmodified tyrosine, it has the smallest volume fraction ($f \approx 0$). CD study reveals that peptide **T1** forms a β-sheet structure (Figure 2a, inset); however, peptide **T1** only forms fibers that are several micrometers in length with no indication of nanoring structure formation (Figure 2a). The width of the fiber (4.8 nm) corresponds well to the height of peptide **T1** (4.7 nm by the CPK model), thereby suggesting that the fibers are typical bilayered β ribbons.[2,21,28] Therefore, this result supports the view that the bulkiness of the dendron segment and resulting steric repulsion effect are responsible for nanoring formation.
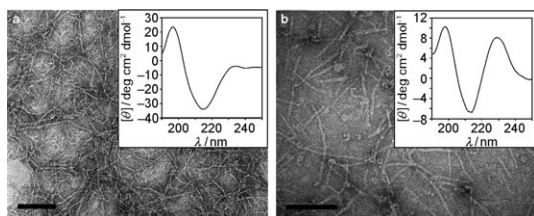

Figure 2. Negative-stain TEM images of a) peptide **T1** and b) peptide **T2**. Bar = 100 nm. Insets: CD spectra of the peptides (20 μM) in 20 mM KF. Abscissa: wavelength [nm]; ordinate: $[\theta] \times 10^{-3}$ [° cm² dmol⁻¹].

To further corroborate the result, we synthesized T-shape peptide **T2** ($f = 0.21$), in which the bulkiness of a dendron segment (first-generation triethylene glycol dendrimer) has been reduced compared to that of nanoring-forming peptide **T3** ($f = 0.47$). CD investigation shows that peptide **T2** also forms a β-sheet structure (Figure 2b, inset). Compared with peptide **T1**, peptide **T2** forms rather short fibrous objects about 100 nm in length as a major population, together with minor nanoring objects (Figure 2b). Similarly to peptide **T1**, the fiber width (4.6 nm) corresponds well to the height of peptide **T2** (4.7 nm), thereby suggesting the formation of β-ribbon structure. These results further emphasize that effective steric repulsion between the dendron segments is crucial for efficient nanoring formation. In addition, weak steric repulsion, although not sufficient to drive efficient nanoring formation, is likely to interfere with 1D fiber growth, thus making the self-assembly process prematurely terminate at an early stage and resulting in the formation of rather short fibers.[29,30] To gain further insight into nanoring formation, we synthesized peptide **T4** ($f = 0.76$), which has a much bulkier hydrophilic dendron (second-generation hexaethylene glycol dendrimer) than that of nanoring-forming peptide **T3**. The results showed that **T4** does not adopt a clearly defined

secondary structure and forms huge irregular aggregates (see the Supporting Information). These results can be interpreted in terms of geometric constraints; the highly bulky dendrons induce excessive curvature at the interface between the peptides, which is not tolerable for a proper β-sheet hydrogen-bonding arrangement. Altogether, these studies indicate that there exists a certain optimal range of dendron bulkiness in which the balance between the curvature induction and the β-sheet formation is delicately controlled.

T-Shape Peptides in a Lipid Bilayer Environment

We next asked the question of whether or not the water-soluble nanorings (β barrels) can be converted into hydrophobic transmembrane β barrels by simple variation in molecular structure. As the thickness of the nanoring (≈ 4 nm) is large enough to span common lipid bilayer membranes (2–4 nm),[31] the transmembrane β barrels, if successfully formed, might act as pores or channels. Studies have shown that, when appropriately designed, various types of organic and inorganic molecules can perform the function of transmembrane pores and channels.[11,15,16,32,33] To enable the outer surface of β barrels to interact with the inner hydrophobic space of a lipid bilayer membrane, a T-shaped building block (peptide **T5**) was designed to have a hydrophobic dendron instead of the hydrophilic oligoether dendrons as in peptides **T3**. The relative volume fraction of the hydrophobic dendron was adjusted to similar levels as peptide **T3** so as to drive efficient nanoring formation (Figure 3a).

Peptide **T5** was barely soluble in water owing to its increased hydrophobicity, but it was clearly soluble in polar organic solvents such as methanol. A CD spectrum of peptide **T5** in methanol shows that the building blocks do not form well-defined secondary structures (Figure 3b). However, a remarkable change in CD spectrum was observed when peptide **T5** was self-assembled in the presence of lipid molecules (Figure 3b). For that experiment, peptide **T5** was mixed with lipid molecules (dioleoyl phosphatidylcholine or DOPC) in methanol/chloroform, the solvents were dried, and the dried film was sonicated in the presence of water following standard liposome preparation protocols (peptide **T5**/DOPC molar ratio = 1:100). As shown in Figure 3b, peptide **T5** adopted a characteristic β-sheet conformation within DOPC liposomes with an intense negative minimum of ellipticity at 216 nm, a strong positive maximum at 197 nm, and a crossover point at 203 nm. This result is in line with a previous report, which showed the potent ability of membranes to promote the secondary structure of β-amyloid peptides and a model hydrophobic hexapeptide.[34,35]

To investigate whether or not the peptide **T5** forms β-barrel pores/channels within the lipid bilayer, we performed a black lipid membrane experiment.[25,26] As illustrated in Figure 3c, a typical current profile was obtained at an applied voltage of +40 mV across the membrane separating 1 M KCl. This step-change behavior offers strong evidence of a single-ion channel.[27] The current (I)/voltage (V) plot in
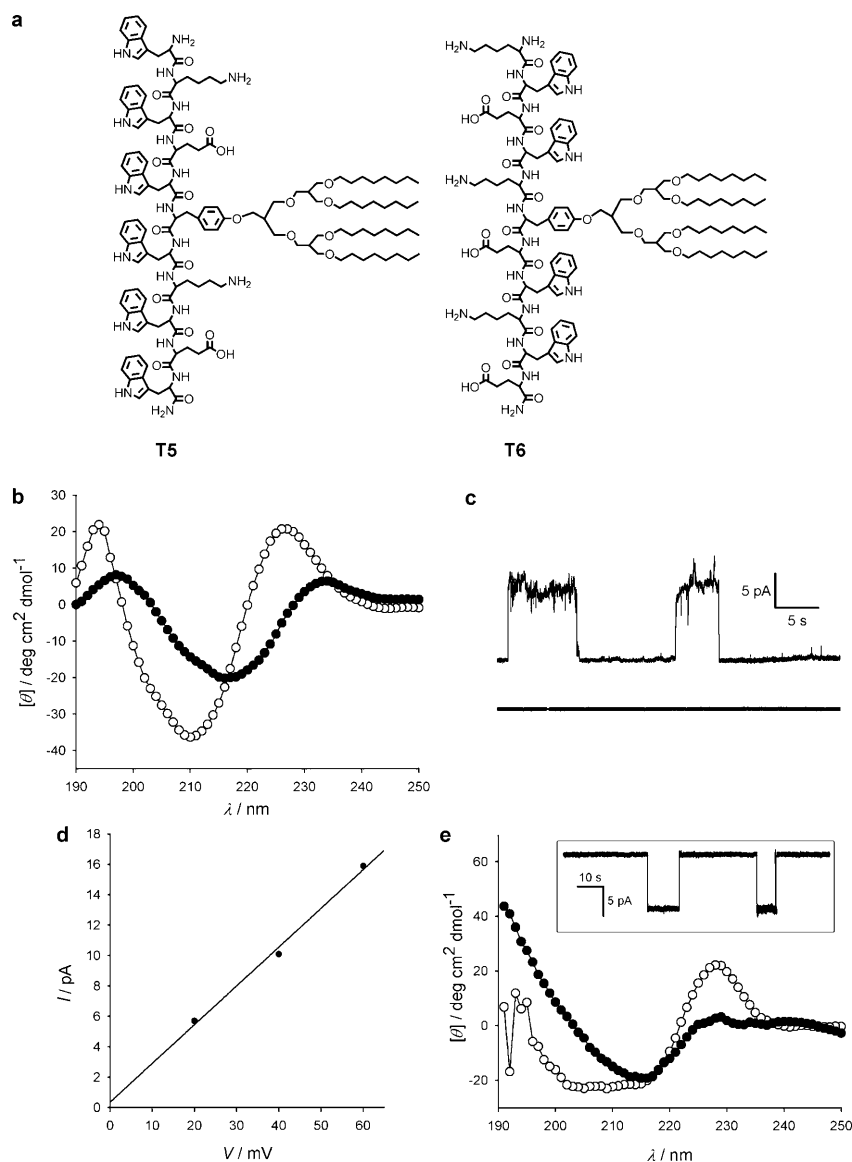
FULL PAPERS

Figure 3. T-shape peptides with hydrophobic dendrons. a) Structures. b) Open circle: a CD spectrum of **T5** (20 μM in methanol). Closed circle: a CD spectrum of **T5** in DOPC liposome (20 μM in water). c) Current profile measured with and without **T5** at +40 mV in 1 M KCl. d) Single-channel *I–V* profile of conductance of **T5** with a linear curve fit. e) Open circle: a CD spectrum of **T6** (20 μM in methanol). Closed circle: a CD spectrum of **T6** in DOPC liposome (20 μM in water). Inset: Current profile measured with **T6**.

from **T5** is incorporated into the lipid membrane and maintains their β-barrel structure so it can transport ions through its pore. Further insight into the pore formation was revealed by an ion-transport assay with a small unilamellar vesicle (SUV) entrapped with pH-sensitive fluorophore HPTS (see the Supporting Information; HPTS = 8-hydroxypyrene-1,3,6-trisulphonic acid). Following peptide **T5** addition at the indicated time point (300 s), the gradual ion transport across the membrane was signaled by the increase in relative fluorescence that accompanied the rise in intravesicular pH.

The molecular arrangement of the peptide segment in **T5** produces a β barrel with hydrophilic amino acid side chains at the outer surface and hydrophobic side chains at the inner surface, which might appear enthalpically unfavorable since the hydrophobic inner surface is exposed to the aqueous environment. Although all the above evidence supports the formation of a β-barrel pore of **T5** in the lipid bilayer, we set out to design more plausible peptide models to further corroborate the ionophore formation. The molecular arrangement of the newly designed peptides (**T6**) can drive the localization of hydrophilic side chains to the inner surface and hydrophobic side chains to the outer surface of β barrels. As shown in Figure 3e, the lipid membrane induced β-sheet formation of otherwise unstructured peptide **T6**. The inset in Figure 3e shows the typical current profile of peptide **T6** across the membrane separating 3 M and 0.2 M KCl. This step-change behavior is strong evidence of a single-ion channel.[37] The β-barrel peptide shows a single-channel current of about 8.7 pA, which corresponds to an ion flux of 5.4×10^7 ions s^{-1}. Interestingly, it shows negative conductivity at this asymmetric condition, which indicates that the pore prefers chloride ion to potassium ion. The results suggest that the amine residues located at the inner surface of the pore play an important role in the anion transport, and the degree of ionization between lysine and glutamic acid resi-

Figure 3 d revealed an ohmic behavior of the ion channel formed by the peptide β barrel, and from the slope, a single-channel conductance of 263 pS was calculated for symmetrical 1 M KCl. The inner-channel diameter can be estimated from the single-channel conductance by using Hille's equation. The corrected Hille diameter $d_{Hille} \approx 0.5$ nm is smaller than the inner diameter (3 nm) of the **T3** nanoring. The smaller diameter is likely to come from the further stabilization of the β-sheet structure owing to mixing of hydrocarbons in dendrons and lipids, which is in line with previous reports that membranes promote secondary-structure formation and self-association of hydrophobic peptides.[34–36] Taken together, we can consider that a nanoring formed

dues is different. Therefore, all the data described above indicate that T-shape building blocks can form β-barrel ionophores when properly designed. More in-depth study on the precise structural requirements for β-barrel ionophore formation should be subject of further investigation.

Conclusion

We have shown how highly versatile peptide-based β-barrel protein mimics with different external and internal surfaces have been developed. The function of the β-barrel mimics can be easily tuned by the simple change in dendron polarity and/or β-sheet peptide configuration. Notably, our design strategy enabled the control of the polarities of the inner surface and outer surface of the β barrels at will. Considering that natural β-barrel proteins consist only of one long polypeptide chain, it is remarkable that simple and relatively small peptide building blocks can mimic natural β-barrel protein folds through a pure noncovalent self-assembly process. Hence, this study lays a foundation for the development of versatile and biocompatible β-barrel protein mimics that can displace the diverse biological functions of natural β-barrel proteins with enhanced properties or with functions unprecedented in nature.

Experimental Section

Peptide was synthesized on Rink amide 4-methylbenzhydrylamine (MBHA) resin with an Applied Biosystems model 433A peptide synthesizer by using standard Fmoc SPPS protocols. Tyrosine derivatives were coupled manually to resin-bound peptide with the *O*-benzotriazole-*N*,*N*,*N'*,*N'*-tetramethyluronium hexafluorophosphate (HBTU) activation method. Standard amino acid protecting groups were employed. For peptide deprotection and cleavage, the resin was treated with cleavage cocktail (trifluoroacetic acid (TFA)/1,2-ethanedithiol/thioanisole: 95:2.5:2.5) for 3 h and was triturated with *tert*-butyl methyl ether. The peptides were purified by reverse-phase high-pressure liquid chromatography (HPLC; water/acetonitrile with 0.1% TFA) on a C4 column (Vydac). The molecular weight was confirmed with MALDI-TOF mass spectrometry. The purity of the peptides was >95% as determined by analytical HPLC. Concentration was determined spectrophotometrically in water/acetonitrile (1:1) urea using a molar extinction coefficient of tryptophan ($5500\,M^{-1}cm^{-1}$) at 280 nm.

For negative stain, the sample (2 μL) was placed onto a carbon-coated copper grid and dried completely. Then 2% (w/v) uranyl acetate solution (2 μL) was added for 1 min and the excess amount of solution was wicked off by filter paper. The cryogenic transmission electron microscopy experiments (cryo-TEM) were performed with a thin film of solution of the peptide (5 μL) transferred to a lacey-supported grid. The thin aqueous films were prepared under controlled temperature and humidity conditions (97–99%) within a custom-built environmental chamber to prevent evaporation of water from sample solution. The excess amount of liquid was blotted with filter paper for 2–3 s, and the thin aqueous films were rapidly vitrified by plunging them into liquid ethane (cooled by liquid nitrogen) at its freezing point. The grid was transferred onto a Gatan 626 cryoholder using a cryotransfer device. After that they were transferred to a JEOL-JEM 2100 TEM instrument. Direct imaging was carried out at a temperature of approximately −175 °C and with a 120 kV accelerating voltage, while acquiring the images with a SC 1000 CCD camera (Gatan, Inc., USA). The data were analyzed with Digital-Micrograph software. Sample concentrations were typically 5–20 μM in

20–150 mM KF. All sample solutions were incubated at least for 2 d at room temperature before transferring to the grid.

The geometry of the polyether group attached to the tyrosine side chain for **T3** was optimized by density functional calculations at the B3LYP/6-31G(d) level. Electrostatic potentials were calculated based on the optimized geometry, and the charges of atoms for the polyether group were obtained through the RESP procedure.[38] The monomer of **T3** was built by linking the polyether group to the original β-sheet peptide (**T1**), whereas the new parameters for the topologies and charges of the polyether group were added to the FF96 force field with the XLEAP program of Amber10. The **T3** monomer was replicated and arranged to make the 12-mer, 24-mer, and 40-mer of the toroidal pore structure with the relative positions of the monomers adjusted to be similar to the structure of antiparallel β sheets. The initial structures were minimized with a limited-memory Bryden–Fletcher–Goldfarb–Shanno quasi-Newton algorithm and heated up to 500 K with the weak-coupling algorithm, whereas the α-carbon atoms were fixed in space. After equilibration at 300 K without the restraints, production molecular dynamic (MD) simulations were performed. For all the computations, the concentration of salt was set as 0.2 M for neutralization and a modified generalized Born model and the FF96 force field with modified hydrogen bonding radii were used.[39]

[1] I. Cherny, E. Gazit, *Angew. Chem.* **2008**, *120*, 4128–4136; *Angew. Chem. Int. Ed.* **2008**, *47*, 4062–4069.

[2] Y. B. Lim, E. Lee, Y. R. Yoon, M. S. Lee, M. Lee, *Angew. Chem.* **2008**, *120*, 4601–4604; *Angew. Chem. Int. Ed.* **2008**, *47*, 4525–4528.

[3] Y. B. Lim, K. S. Moon, M. Lee, *Chem. Soc. Rev.* **2009**, *38*, 925–934.

[4] R. J. Mart, R. D. Osborne, M. M. Stevens, R. V. Ulijn, *Soft Matter* **2006**, *2*, 822–835.

[5] T. Jovanovic-Talisman, J. Tetenbaum-Novatt, A. S. McKenney, A. Zilman, R. Peters, M. P. Rout, B. T. Chait, *Nature* **2009**, *457*, 1023–1027.

[6] E. Mastrobattista, M. A. van der Aa, W. E. Hennink, D. J. Crommelin, *Nat. Rev. Drug Discovery* **2006**, *5*, 115–121.

[7] V. Zeevi, A. Tovkach, T. Tzfira, *Proc. Natl. Acad. Sci. USA* **2008**, *105*, 12785–12790.

[8] R. K. Wierenga, *FEBS Lett.* **2001**, *492*, 193–198.

[9] W. C. Wimley, *Curr. Opin. Struct. Biol.* **2003**, *13*, 404–411.

[10] N. Sakai, J. Mareda, S. Matile, *Acc. Chem. Res.* **2005**, *38*, 79–87.

[11] N. Sakai, J. Mareda, S. Matile, *Acc. Chem. Res.* **2008**, *41*, 1354–1365.

[12] A. L. Sisson, M. R. Shah, S. Bhosale, S. Matile, *Chem. Soc. Rev.* **2006**, *35*, 1269–1286.

[13] M. S. Kaucher, M. Peterca, A. E. Dulcey, A. J. Kim, S. A. Vinogradov, D. A. Hammer, P. A. Heiney, V. Percec, *J. Am. Chem. Soc.* **2007**, *129*, 11698–11699.

[14] A. J. Kim, M. S. Kaucher, K. P. Davis, M. Peterca, M. R. Imam, N. A. Christian, D. H. Levine, F. S. Bates, V. Percec, D. A. Hammer, *Adv. Funct. Mater.* **2009**, *19*, 2930–2936.

[15] V. Percec, A. E. Dulcey, V. S. K. Balagurusamy, Y. Miura, J. Smidrkal, M. Peterca, S. Nummelin, U. Edlund, S. D. Hudson, P. A. Heiney, D. A. Hu, S. N. Magonov, S. A. Vinogradov, *Nature* **2004**, *430*, 764–768.

[16] M. R. Ghadiri, J. R. Granja, R. A. Milligan, D. E. Mcree, N. Khazanovich, *Nature* **1993**, *366*, 324–327.

[17] W. Y. Yang, J. H. Ahn, Y. S. Yoo, N. K. Oh, M. Lee, *Nat. Mater.* **2005**, *4*, 399–402.

FULL PAPERS

[18] A. J. Baldwin, R. Bader, J. Christodoulou, C. E. MacPhee, C. M. Dobson, P. D. Barker, *J. Am. Chem. Soc.* **2006**, *128*, 2162–2163.

[19] A. M. Squires, G. L. Devlin, S. L. Gras, A. K. Tickler, C. E. Mac-Phee, C. M. Dobson, *J. Am. Chem. Soc.* **2006**, *128*, 11738–11739.

[20] Y. B. Lim, M. Lee, *J. Mater. Chem.* **2008**, *18*, 723–727.

[21] D. M. Marini, W. Hwang, D. A. Lauffenburger, S. G. Zhang, R. D. Kamm, *Nano Lett.* **2002**, *2*, 295–299.

[22] K. Matsuura, K. Murasato, N. Kimizuka, *J. Am. Chem. Soc.* **2005**, *127*, 10148–10149.

[23] T. S. Burkoth, T. L. S. Benzinger, D. N. M. Jones, K. Hallenga, S. C. Meredith, D. G. Lynn, *J. Am. Chem. Soc.* **1998**, *120*, 7655–7656.

[24] J. Hentschel, E. Krause, H. G. Börner, *J. Am. Chem. Soc.* **2006**, *128*, 7722–7723.

[25] T. Beke, I. G. Csizmadia, A. Perczel, *J. Am. Chem. Soc.* **2006**, *128*, 5158–5167.

[26] T. Beke, A. Czajlik, B. Balint, A. Perczel, *ACS Nano* **2008**, *2*, 545–553.

[27] D. Dieudonné, A. Gericke, C. R. Flach, X. Jiang, R. S. Farid, R. Mendelsohn, *J. Am. Chem. Soc.* **1998**, *120*, 792–799.

[28] Y. B. Lim, E. Lee, M. Lee, *Angew. Chem.* **2007**, *119*, 3545–3548; *Angew. Chem. Int. Ed.* **2007**, *46*, 3475–3478.

[29] H. Dong, S. E. Paramonov, L. Aulisa, E. L. Bakota, J. D. Hartgerink, *J. Am. Chem. Soc.* **2007**, *129*, 12468–12472.

[30] Y. B. Lim, S. Park, E. Lee, H. Jeong, J. H. Ryu, M. S. Lee, *Biomacromolecules* **2007**, *8*, 1404–1408.

[31] L. K. Tamm, A. Arora, J. H. Kleinschmidt, *J. Biol. Chem.* **2001**, *276*, 32399–32402.

[32] A. J. Helsel, A. L. Brown, K. Yamato, W. Feng, L. Yuan, A. J. Clements, S. V. Harding, G. Szabo, Z. Shao, B. Gong, *J. Am. Chem. Soc.* **2008**, *130*, 15784–15785.

[33] M. Jung, H. Kim, K. Baek, K. Kim, *Angew. Chem.* **2008**, *120*, 5839–5841; *Angew. Chem. Int. Ed.* **2008**, *47*, 5755–5757.

[34] E. Terzi, G. Holzemann, J. Seelig, *J. Mol. Biol.* **1995**, *252*, 633–642.

[35] W. C. Wimley, K. Hristova, A. S. Ladokhin, L. Silvestro, P. H. Axelsen, S. H. White, *J. Mol. Biol.* **1998**, *277*, 1091–1110.

[36] E. Terzi, G. Holzemann, J. Seelig, *Biochemistry* **1997**, *36*, 14845–14852.

[37] T. M. Fyles, *Chem. Soc. Rev.* **2007**, *36*, 335–347.

[38] W. D. Cornell, P. Cieplak, C. I. Bayly, P. A. Kollman, *J. Am. Chem. Soc.* **1993**, *115*, 9620–9631.

[39] M. Feig, A. Onufriev, M. S. Lee, W. Im, D. A. Case, C. L. Brooks, III, *J. Comput. Chem.* **2004**, *25*, 265–284.